Proceedings of CONF-MPCS 2026 Symposium: Theoretic Physics and Plasma Physics
DOI: 10.54254/2753-8818/2026.DL32571

CFD Simulation and Experimental Verification of Spiral Propulsion Performance in Low Reynolds Number Based on Scale Model

Yizhe Wang

ZJU-UIUC Institute, Zhejiang University, Hangzhou, China
3126375913@qq.com

Abstract. Study of low Reynolds number flow environments are very practical in microfluidic systems, biological fluid scenarios, and micro underwater vehicles. Due to the influence of fluid viscosity, traditional propeller propulsion mechanisms completely fail in this environment. The spiral flagellar structure inspired by microorganisms can achieve stable propulsion in low Reynolds number fluids. However, the verification of its related theoretical models still lacks sufficient experimental support, and existing research mostly focuses on numerical theoretical derivation. Therefore, this article takes the mathematical model proposed by Lauga and Magariyama etc. of the spiral flagellar propulsion effect of micro robots in low Reynolds number fluids as the research object. Using both CFD simulation and real built robot to verify the model. The research results indicate that the result obtained from CFD simulation is highly consistent with the mathematical model proposed by Lauga and Magariyama. And the physical model further verified the rationality of the theoretical model. The research results can provide direct experimental basis for the design and optimization of biomimetic spiral flagellar propulsed robot in low Reynolds number environment.

Keywords: Low Reynolds Number Flow, Helical Flagellar Propulsion, CFD Simulation, Resistive Force Theory, Scaled Model Experiment

1. Introduction

Low Reynolds number (Re number) environments are widely present in microfluidic systems, biological fluid environments, and micro underwater vehicles [1]. In this environment, traditional propeller propulsion mechanisms fail due to the flow characteristics dominated by fluid viscosity [2,3].

However, as an efficient propulsion structure evolved by microorganisms such as bacteria [4] and sperm [5], spiral flagella [6], with their unique rotation motion mode, can achieve stable propulsion in low Reynolds number fluids [7]. Its earliest observations can be traced back to the 18th century [8]. And it also has become a most popular aspect of biological research recently [1]. It is an important blueprint for biomimetic low Reynolds number propulsion technology as well [9]. Exploring the propulsion effect of helical tail in low Reynolds number fluids can not only reveal the

© 2026 The Authors. This is an open access article distributed under the terms of the Creative Commons Attribution License 4.0 (https://creativecommons.org/licenses/by/4.0/).

DOI: 10.54254/2753-8818/2026.DL32571

kinematic feature of microorganisms in nature but also provide core theoretical support for the design and optimization of micro biomimetic propulsion devices, which have important practical application value in microsurgery [10], medicine delivery [11], water purification [12] and so on.

To study the performance of a helix tail, infinitesimal method is a good way to simplify the problem. A helix filament can be divided into small slender filaments with small deformation [13]. And the propulsion force can be calculated using the Slender-body theory [14]. With some further derivation on relationship between rotational speed, propulsion force and resistant force, a mathematical model of the helix tail can be built [15]. However, past researches mostly focused on numerical derivation and lack of computer simulation and real experiments [16]. Thus, our research aims to verify the mathematical model of the propulsion effect of helical filaments of a micro robot in low Re Number fluids using both CFD simulations and real tests.

Scaled models are a good way to study performance of a microstructure. Some research has already proved the reliability of a macroscopic scale model using in study about the performance of small flagellar [17]. The key point for building a scaled model in fluid mechanics is to keep the Re number unchanged. In the research, the micro robot was magnified to centimeter level while keeping the Re number low enough. This gives us a much easier way to investigate the performance of helical filaments.

Our research can provide direct experimental basis for the design of biomimetic low Reynolds number spiral propulsion robots, and feasible experimental ideas for the development of micro propulsion devices in high viscosity and low Reynolds number environments.

2. Result

In Lauga's paper, to calculate the drag force of those small slender filaments, he first ignores the small deformation of those filaments and uses several lined spheres to modelized the small rod. He uses Stokes equation to calculate the drag force of each sphere and integrate to get the total drag force of the filaments both along the rod and perpendicular to the rod direction. And finally, he uses a correction formula to incorporate these small deformations. However, the model he uses to find out the drag force of the slender filaments is not so accurate but more based on physical intuition. So, a CFD test using COMSOL software was conducted to test his theory.

2.1. CFD test for propulsion force

In the CFD test, a rectangle with length of 1cm and width with 1mm was used to present one slender filament in 2 dimensions and calculate the performance of the fluids in a square with side length of 0.5m to avoid boundary effect. The fluid with density of $1.23*10^3\ kg/m^3$ and dynamic viscosity of 800 mPa*s flow to +x direction in room temperature. The testing mesh grid looks like part (a) of Figure 1 below. There are more grid points near the testing body in order to get a more precise result. After simulation, the flow field with initial flow speed of 0.005m/s is shown in part (b) of Figure 1.

DOI: 10.54254/2753-8818/2026.DL32571

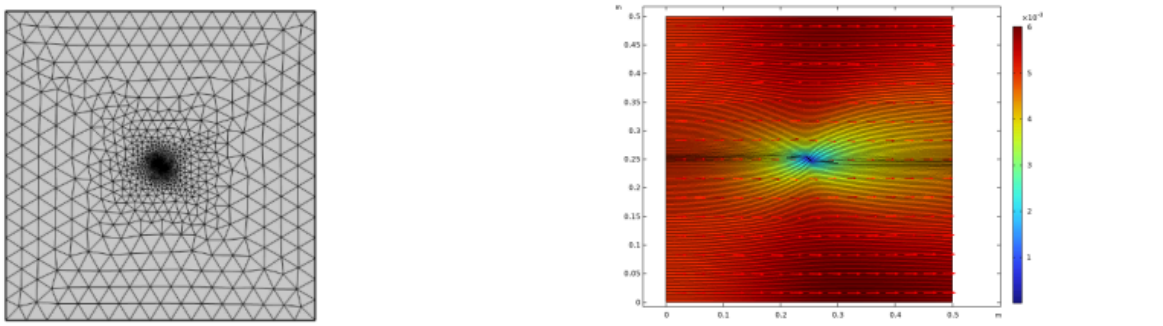

(a) Grid network for CFD simulation (b) Flow Field with initial flow speed of 0.005m/s

Figure 1. Setup for CFD simulation of tail

The red arrow shows the flow direction at each point, and the color of the background shows the flow speed of the fluid. The drag force on the filament in y direction, which is named propulsion force since it is the force that propulse the helix, was calculated using integration tool in the software. And after scanning the speed between 1 mm/s to 5 mm/s with steps of 0.2 mm/s, the software gives the data in Figure 2.

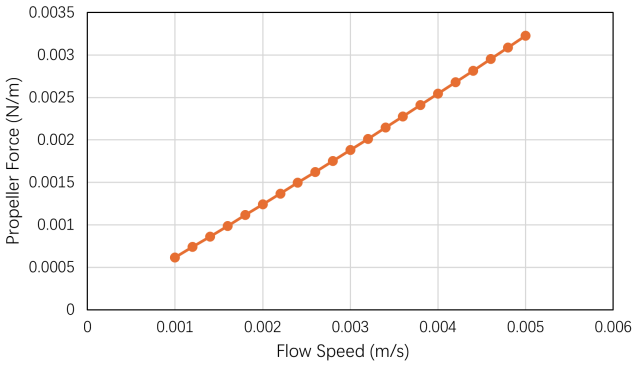

Figure 2. Propeller force versus flow speed

It is easy to say that the CFD result shows a linear relationship between the propulsion force and the flow speed,

$$f_{prop} = 0.6527u - 6*10^{-5} \tag{1}$$

with $R^2 = 0.9997$. Here f_{prop} is the propeller force generated by this small filament and u is the flow speed of the direction that is perpendicular to the force.

R^2 is a statistical indicator used to indicate the fitting wellness. The closer the indicator to 1 the better the fitting is.

Equation (1) can be regarded as proportional relationship with such a small y-axis intercept. Though the CFD was done on a 2D cross section of the whole filament body, it still can present the relationship between the propulsion force on whole 3D body and the flow speed. And this relationship matches well with the equation in Lauga's paper,

$$f_{prop} = (\xi_{||} - \xi_{\perp}) u \, sin\,\theta \, cos\,\theta \, e_x \tag{2}$$

DOI: 10.54254/2753-8818/2026.DL32571

where $\xi_{||}$ and $\xi_{\perp}$ are the corresponding drag coefficients. u and θ are the speed and the direction of the flow.

Both equation (1) and (2) all show a proportional relationship between speed and propulsion force. They proved that the instinct model of the filament body that given by Lauga matches well with the real situation.

In the real helix propeller, the speed which generates the propulsion force is in fact caused by rotation. And after doing the integration, these equations are gotten [15],

$$F_{propeller} = \gamma_f{}^{*}\omega_f \tag{3}$$

$$\gamma_f = \frac{2\pi\mu L}{\left(\ln\left(\frac{d}{2p}\right)+1/2\right)\left(4\pi^2r^2+p^2\right)} * \left(-2\pi r^2 p\right) \tag{4}$$

where ω_f is Rotation rates of flagellar filament, $2d$ is the diameter of flagellar filament, L is the length of flagellar filament, p is the pitch of flagellar helix, r is the radius of flagellar helix, μ is the viscosity of fluid and γ_f is the drag coefficients of flagellar filament.

To further test the performance of the helix propeller in real environment, a robot model was built. The robot had an ellipse head made of 3D printing resin and helix tail made of iron wire. A gear motor was used to connect the head with the tail and provide rotational force to the tail. And the whole robot model was powered by a button cell. To simulate the low Re number environment of the robot, the model was put into the laundry detergent, which had a higher viscosity, in the experiment.

The Magariyama's paper tells that the speed of the robot depends on the drag force, the fluid acting on both the head and the tail and the propulsion force generated by the tail and basically meet the following three formulas [15]:

$$F_c + F_f = 0 \tag{5}$$

$$F_c = \alpha_c v \tag{6}$$

$$F_f = F_{f\_swim} + F_{propeller} \tag{7}$$

$$F_{f\_swim} = \alpha_f v \tag{8}$$

where F_c and F_f are hydrodynamic force acting on cell body and flagellar filament, F_{f_swim} is the drag force acting on the tail that is caused by robot swimming, α_f and α_c are drag coefficients of flagellar filament and cell body that defined in Magariyama's paper, and v is the swimming speed of the robot.

However, it is necessary to do some tests to verify the accuracy of the equation (5)-(7). The equation of the propulsion force, which is $\gamma_f\omega_f$ in this formula, has already been proved using computer simulation. Now another CFD test was needed to learn the relationship between the drag force and the speed.

DOI: 10.54254/2753-8818/2026.DL32571

2.2. CFD test for drag force

2.2.1. Drag force of the tail

The CFD test on the drag force of the tail performs almost the same as the test of propulsion force. But in the last step, rather than drag force in y direction is recorded, the drag force in x direction is recorded this time. And here in Figure 3 is the result data.

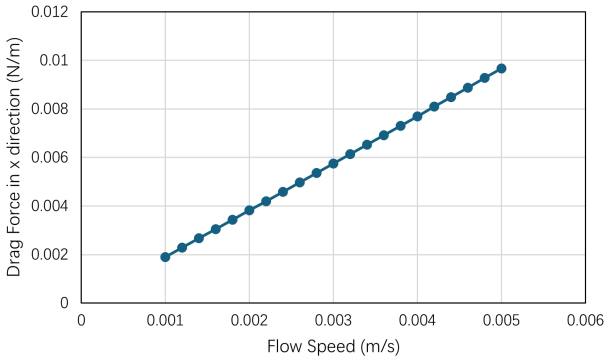

Figure 3. Drag force on tail versus flow speed

This shows the drag force in x direction also shows a linear relationship with flow speed. And the equation is,

$$F_{f\_swim} = 1.9417u - 6*10^{-5} \tag{9}$$

with $R^2 = 1$.

Such a small y-axis interception in equation (9) means the drag force caused by robot swimming shows a proportional relationship with the swimming speed, which matches the inference in Magariyama's paper shows in equation (8).

2.2.2. Drag force of the head

Then for the simulation about the head of the robot. The ellipsoid body was projected the into an ellipse with semi-major axis of 0.045m and semi-minor axis of 0.015m in 2D plane. Since the head is much bigger than the small filament used in propulsion test. A bigger region (0.5m x 0.8m) of testing fluid was used to avoid boundary effects. Here in Figure 4 is the mesh grid figure and flow field with initial flow speed of 0.005m/s.

DOI: 10.54254/2753-8818/2026.DL32571

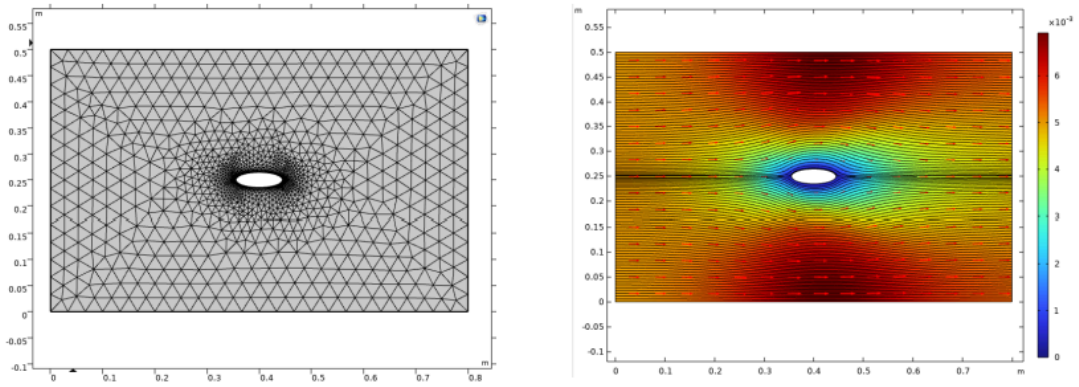

(a) Grid network for CFD simulation (b) Flow Field with initial flow speed of 0.005m/s

Figure 4. Setup for CFD simulation of head

And a scan was conducted from 0.001 m/s to 0.005 m/s with steps of 0.0002 m/s to find the relationship between moving speed to the drag force. The result is shown in the Figure 5.

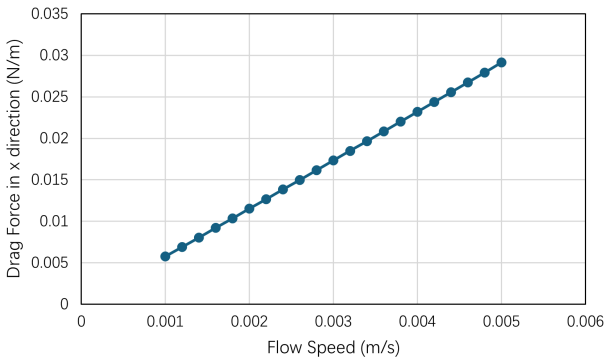

Figure 5. Drag force on tail versus flow speed

It shows that the drag force acting on head and the flow speed meets a linear relationship with equation of,

$$F_c = 5.8392u - 0.0002 \tag{10}$$

with $R^2 = 1$.

Also, after ignoring the small y-axis interception in equation (10), the relationship matches the relationship shows in equation (6).

2.3. A robot to verify the CFD simulation result in real world

As the simulation have already proved the equations of drag force and propulsion force in Magariyama's paper. His formula can be used to predict the performance of the robot. Since the propulsion force only relates to the rotational speed of the tail, and the resistance force all comes from the drag force that related to the moving speed of the robot. A direct proportional relationship between rotational speed and moving speed was expected.

Our robot model's head is designed in a size of 4.5 cm on semi-major axis and 1.5 cm on the other semi axis. And the tail has the size of 10 cm long, 3 cm radius and 45 degrees pitch angel. The

DOI: 10.54254/2753-8818/2026.DL32571

diameter of the iron wire that makes the tail is about 1 mm. And the motor is designed to rotate at a speed of 1 Hz, 2Hz, 5Hz, 8.3Hz and 10Hz. The robot is moving in laundry detergent with density about 1.23e3 kg/m^3 and viscosity about 2000mPa. This design allowed us to study the moving speed of the robot with different rotational speed in the environment of about 1-2 Re number. In Figure 6 is a photo of the robot during the experiment.

Figure 6. A photo of the robot moving in laundry detergent

The experiment gives us the data shows in Table 1 and Figure 7.

Table 1. Data of the robot test

Rotational Speed (Hz)	Moving Speed (mm/s)
1	1
2	1.5
5	2.5
8.33	4
10	6

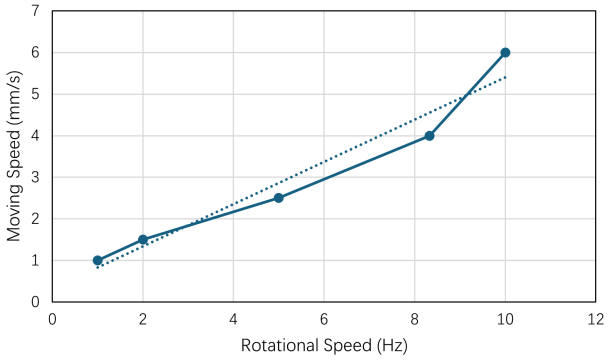

Figure 7. Moving speed of the robot versus rotational speed of the tail

DOI: 10.54254/2753-8818/2026.DL32571

It is easy to observe that the moving speed of the robot model is increasing linearly with the increase of the rotational speed of the tail with equation of,

$$v = 0.5508\omega_f \tag{11}$$

with $R^2 = 0.9835$. And it matches prediction.

3. Conclusion

The result suggests that as long as the rotational speed of the tail is increased, the robot will move as quickly as possible. This seems to approve with the theoretical expectation that the moving speed of the robot is directly proportional to the rotational speed of the tail [15].

However, the data in the experiment seems not to completely agree with the calculated data. The moving speed of the robot in the real experiment is significantly lower than the expected speed calculated by Magariyama's equations. Through analysis, this can be caused by following results.

First, the rotational speed of the tail may not be as high as the design. There is some unexpected friction, like the friction between the rotation axis and the shell of the robot, in the model. This will cause a decrease in the rotational speed of the motor and thus the moving speed will be lower than expected.

Second, due to the device limitation, measuring speed by using timer and ruler is not so accurate and will cause some errors to the result.

Third, the viscosity data used in calculation is an average number of this brand of laundry detergent. But the real viscosity of the laundry detergent that was used in the experiment has not been measured. Its viscosity may be lower than the average and this may cause the unexpected moving speed.

Though there are some errors, our experiment can still prove that the RFT model used in both Lauga and Magariyama's paper can reflect the real situation perfectly. Further study can be conducted to verify the model more precisely.

References

[1] Ganguly S, M KR. Hydrodynamics of squirmers: A review on Stokesian principles, analytical frameworks, and recent advances. Phys Fluids 2025; 37: 121304.
[2] Ishimoto K, Yamada M. A Coordinate-Based Proof of the Scallop Theorem. SIAM J Appl Math 2012; 72: 1686–1694.
[3] Purcell E. Life at Low Reynolds Number.
[4] Macnab RM. Bacterial flagella rotating in bundles: a study in helical geometry. Proc Natl Acad Sci 1977; 74: 221–225.
[5] Gray J. The Movement of Sea-Urchin Spermatozoa. J Exp Biol 1955; 32: 775–801.
[6] Yates GT. How Microorganisms Move through Water: The hydrodynamics of ciliary and flagellar propulsion reveal how microorganisms overcome the extreme effect of the viscosity of water. Am Sci 1986; 74: 358–365.
[7] Guasto JS, Rusconi R, Stocker R. Fluid Mechanics of Planktonic Microorganisms. Annu Rev Fluid Mech 2012; 44: 373–400.
[8] Thormann KM, Beta C, Kühn MJ. Wrapped Up: The Motility of Polarly Flagellated Bacteria. Annu Rev Microbiol 2022; 76: 349–367.
[9] Zhang L, Peyer KE, Nelson BJ. Artificial bacterial flagella for micromanipulation. Lab Chip 2010; 10: 2203.
[10] Edd J, Payen S, Rubinsky B, et al. Biomimetic propulsion for a swimming surgical micro-robot. In: Proceedings 2003 IEEE/RSJ International Conference on Intelligent Robots and Systems (IROS 2003) (Cat. No.03CH37453), pp. 2583–2588 vol.3.
[11] Patra D, Sengupta S, Duan W, et al. Intelligent, self-powered, drug delivery systems. Nanoscale 2013; 5: 1273–1283.

DOI: 10.54254/2753-8818/2026.DL32571

[12] Liu J, Fu Y, Liu X, et al. Theoretical Perspectives on Natural and Artificial Micro-swimmers. Acta Mech Solida Sin 2021; 34: 783–809.
[13] Lauga E, Powers TR. The hydrodynamics of swimming microorganisms. Rep Prog Phys 2009; 72: 096601.
[14] Batchelor GK. Slender-body theory for particles of arbitrary cross-section in Stokes flow. J Fluid Mech 1970; 44: 419–440.
[15] Magariyama Y, Kudo S. A Mathematical Explanation of an Increase in Bacterial Swimming Speed with Viscosity in Linear-Polymer Solutions. Biophys J 2002; 83: 733–739.
[16] Pak OS, Lauga E. Theoretical models in low-Reynolds-number locomotion. Epub ahead of print 16 October 2014. DOI: 10.48550/arXiv.1410.4321.
[17] Kim M, Bird JC, Van Parys AJ, et al. A macroscopic scale model of bacterial flagellar bundling. Proc Natl Acad Sci 2003; 100: 15481–15485.